NASA Technical Memorandum 105313

# Computational Simulation of Surface Waviness in Graphite/Epoxy Woven Composites Due to Initial Curing

Jose G. Sanfeliz, Pappu L.N. Murthy,
and Christos C. Chamis
*Lewis Research Center*
*Cleveland, Ohio*

**NASA**

ERRATA

NASA Technical Memorandum 105313

COMPUTATIONAL SIMULATION OF SURFACE WAVINESS IN GRAPHITE/EPOXY
WOVEN COMPOSITES DUE TO INITIAL CURING

Jose G. Sanfeliz, Pappu L.N. Murthy, and Christos C. Chamis
National Aeronautics and Space Administration
Lewis Research Center
Cleveland, Ohio 44135

Replace pages 3 through 7 with revised pages 3 through 7.

# COMPUTATIONAL SIMULATION OF SURFACE WAVINESS IN GRAPHITE/EPOXY WOVEN COMPOSITES DUE TO INITIAL CURING

Jose G. Sanfeliz, Pappu L.N. Murthy, and Christos C. Chamis
National Aeronautics and Space Administration
Lewis Research Center
Cleveland, Ohio 44135

## ABSTRACT

Several models simulating plain weave, graphite/epoxy woven composites are presented, along with the effects that the simultaneous application of pressure and thermal loads have on their surfaces. The surface effects created by moisture absorption are also examined. The computational simulation consisted of using a two-dimensional finite element model for the composite. The properties of the finite element (FE) model are calculated by using the in-house composite mechanics computer code ICAN (Integrated Composite ANalyzer). MSC/NASTRAN is used for the FE analysis which yields the composite's top surface normalized displacements. These results demonstrate the importance of parameters such as the cure temperature ($T_o$) and the resin content in the curing process of polymer-matrix composites. The modification of these parameters will help tailor the composite system to the desired requirements and applications.

KEY WORDS: Composite Materials; Woven Composites; Curing Process; Epoxy Resin; Print-through; Fiber Volume Ratio; Thermal Expansion Coefficient; Moisture Expansion Coefficient; Finite Element Analysis.

## 1. INTRODUCTION

Woven fiber composites are among the most used fiber reinforced resin matrix systems for aerospace applications. They have many advantages over laminates made from individual layers of unidirectional material. These advantages are: (1) Improved formability and drape, (2) bidirectional reinforcement in a single layer, (3) improved impact resistance, and (4) balanced properties in the fabric plane (ref. 1). A woven fiber arrangement is formed by interlacing two sets of yarns, the warp yarns or ends and the filling yarns or picks. The warp yarns lie in the lengthwise direction of the fabrics, whereas the filling yarns lie at right angles to the warp yarn. These fibers can be woven into many types of weave patterns, width, and thicknesses, each having its own structural characteristics. Figure 1 depicts schematics of laminae with unidirectionally aligned fibers and woven fabric. Graphite/epoxy woven composites are subjected to a curing process which transforms the soft and flexible resin-impregnated fibers into a stiff, usable structural material. The curing process involves the simultaneous application of heat and pressure for predetermined periods of time. The temperatures applied during the cure provide the heat required for initiating and maintaining the chemical reactions in the resin which cause the desired changes in the molecular structure. The applied pressure provides the force needed to squeeze excess resin out of the material and to consolidate individual plies (ref. 2). Due to the cooling process to room temperature, the composite's surface develops wrinkles because of the local differences in the thermal expansion coef-

ficients of resin rich and fiber rich areas of the composite system. This phenomenon is known as print-through (ref. 3). Even though the waviness of the woven composite's surface is not considered important for most structural applications, such is not the case for applications to solar dynamic concentrators made from graphite fiber/epoxy composites. The quality and smoothness of the composite mirror's surface is critical and is affected by changes in the dimension of the epoxy during the curing process. The surface wrinkles can also be developed by the presence of moisture in the composite. The epoxy resin is sensitive to the application of hygral loads, causing its properties to change considerably. This event will affect the resin rich areas of the woven composite system.

The objectives of this paper are: (1) Create models that will simulate woven graphite/epoxy composites (plain weave fabric construction) and (2) investigate the initial effects of curing and moisture on the top surface of graphite/epoxy woven composites. These effects will be measured by the values of the composites' surface normalized displacements ($\delta$) obtained from a finite element (FE) analysis using MSC/NASTRAN.

## 2. GENERAL ASSUMPTIONS

The following assumptions will be used throughout the analysis of the composite models:

1. The models used to examine the initial curing effects will be subjected to a cure pressure of $P_0$ = 293.25 kPa (42.5 psi) and a cure temperature $T_0$ = 180 °C (355 °F). Both of these values are arbitrary. Several researchers have performed tests on graphite/epoxy composites with cure pressures ranging from 103 kPa (15 psi) to 724.5 kPa (105 psi) and a cure temperature limit of 180 °C (355 °F) (ref. 2).

2. A moisture content of 1 percent will be used to analyze the effects of this load on the woven composite models. The hygral load will be applied separately from the cure temperature and pressure.

3. The FE models (figures 2(a) and (b)) represent a cross section of a typical composite being subjected to the loading conditions described in assumptions 1 and 2, respectively. The models are also restrained around the sides, preventing any extension in the Y direction. The through-the-thickness direction is denoted by the letter Z.

4. The process of curing epoxy resins is, in general, time-dependent and nonlinear. Experimental results on resin matrix composites such as boron/epoxy and graphite/epoxy indicate that as a first approximation these composites can be assumed to behave elastically (ref. 4). This means that the history has no effect on the present material, hence, a time-independent, linear analysis can be performed to study their initial behavior.

2

# 3. WOVEN COMPOSITE MODELS

There are two main factors that need to be considered in the analysis and modelling of woven composites: (1) Due to the local fiber arrangement, the fiber volume ratio $(k_f)$ is not likely to be as uniform as that for unidirectional and cross-ply composites and (2) the fibers must cross over one another. Both of these factors will be examined in the following models. The woven composite model is simulated by examining the two representative regions depicted in figure 3. Region A represents a cross section where the warp and filling yarns cross over one another while region B isolates a matrix rich section of the plain weave woven composite. Region A is divided into three uniform sections as shown in figure 4(a). Section 1 consists of a filling yarn and part of a warp yarn crossing over the filling yarn. Section 2 consists only of the warp yarn as it travels across the representative volume. For modelling purposes, section 1 will be simulated by considering material properties corresponding to a [0/90] graphite/epoxy composite while sections 2 will be represented by considering [+45] and [-45] graphite/epoxy composite properties. The 45° approximation in section 2 was assumed since the length of each fiber is affected by the undulations created as the fibers cross over one another. Because the analysis considers the same representative volume, each section of the composite is assumed to be of the same width. The width of each section is equal to 1, therefore the length of the fibers in section 2 $(l_2)$ is equal to $(2)^{1/2}l$. The thickness of the ply is t, where $t \geq l$ and the diameter of the graphite fiber bundle for each section is equal to D. These dimensions are depicted in figure 4(b). Region B (figure 4(c)) is also divided into three uniform sections. Section 3 consists of a fiber bundle of diameter D and matrix material. This section will be simulated by considering the material properties of an unidirectional composite with an interply matrix layer. Section 4 consists locally of only matrix material (epoxy resin). The composite properties for each section of regions A and B are determined by their fiber content, that is, their fiber volume ratios. The $k_f$ calculations are based on the geometric parameters that define each section of the woven composite. The volume of the fibers in section 1, region A is calculated as:

$$V_{f1} = \frac{\pi D^2}{4}(1) + \frac{\pi D^2}{4}(1 + 2l_2) \tag{1}$$

where D is the diameter of the fiber bundle, 1 is the width of the composite section, and $l_2$ is the length of each diagonal fiber in the representative volume. The representative volume (V) for each composite section is equal to (1) x (t) x (31), which yields:

$$V = 3l^2 t \tag{2}$$

The contribution of the diagonal fibers to the volume of section 1 is clearly shown in figure 3. Since the length of these fibers $(l_2)$ is assumed to be equal to $(2)^{1/2}l$, from equation (1) the volume of the fibers is equal to:

3

$$V_{f1} = \frac{\pi D^2}{4}(2l + 2\sqrt{2}l) = \frac{\pi D^2}{2}l(1 + \sqrt{2}) \tag{3}$$

Hence, the fiber volume ratio of section 1 is calculated as:

$$k_{f1} = \frac{V_{f1}}{V} = \frac{\pi D^2(1 + \sqrt{2})}{6lt} \tag{4}$$

The fiber volume ratio of section 2 is calculated in a similar manner. The volume of the fibers in this section is given by the following equation:

$$V_{f2} = \frac{\pi D^2}{4}(l_2) \tag{5}$$

where, again, $l_2$ is the length of the diagonal fiber. Since section 2 contains the same representative volume as section 1, the fiber volume ratio of section 2 is obtained as:

$$k_{f2} = \frac{V_{f2}}{V} = \frac{\frac{\pi D^2}{4}l\sqrt{2}}{3l^2 t} = \frac{\pi D^2\sqrt{2}}{12lt} \tag{6}$$

Taking the ratio of equation (4) over equation (6), the following relationship between the $k_f$'s of sections 1 and 2 is obtained:

$$\frac{k_{f1}}{k_{f2}} = \frac{\pi D^2(1 + \sqrt{2})}{6lt}\frac{12lt}{\pi D^2\sqrt{2}} = \frac{2(1 + \sqrt{2})}{\sqrt{2}} = 3.4 \tag{7}$$

that is, the fiber content of section 1 (fiber rich section) is over 3 times the fiber content of section 2.

The fiber volume ratio calculations in region B (see figure 3) only involve section 3 since it is assumed that locally, section 4 is only matrix ($k_{f4} = 0$). The volume of the fibers in section 3 is calculated as:

$$V_{f3} = \frac{\pi D^2}{4}(2l + l_2) = \frac{\pi D^2}{4}l(2 + \sqrt{2}) \tag{8}$$

Again, since each section consists of the same representative volume (V), the fiber volume ratio of section 3 is given by:

$$k_{f3} = \frac{V_{f3}}{V} = \frac{\pi D^2(2 + \sqrt{2})}{12lt} \tag{9}$$

4

The ratio of equations (4) over (9), which relates the $k_f$'s of sections 1 and 3, yields the following:

$$\frac{k_{f1}}{k_{f3}} = \frac{2(1+\sqrt{2})}{(2+\sqrt{2})} = 1.4 \tag{10}$$

This result is expected since the length of the fibers in section 3 is less than in section 1, i.e., $(2 + (2)^{1/2})$ 1 < $2(1 + (2)^{1/2})$ 1. Therefore, $k_{f1}$ should be greater than $k_{f3}$. Both equations (7) and (10) define the relationships needed to obtain the fiber volume ratio combinations for the alternate sections of regions A and B. Given the $k_f$ of any section of the composite, the fiber volume ratios for each fiber and matrix rich section are calculated. The corresponding material properties for these alternate sections are also obtained.

The material properties are computed for each fiber volume ratio case using the computer program ICAN (ref. 5). ICAN (Integrated Composite ANalyzer) is an in-house computer code developed by the Structural Mechanics Branch at NASA Lewis Research Center, which incorporates micromechanical and laminate analysis capabilities for the simulation of polymer-matrix composites. The calculated composite properties are subsequently used to define element properties in the FE analysis. The finite element model consists of 104 CQUAD4 elements as shown in figures 5(a) and (b). Figure 5(a) represents the alternate cross sections of the woven composite defined by region A, the region where the fibers cross over one another. Figure 5(b) represents the alternate cross sections defined by region B. Out of the 104 elements, 52 elements from the top half of the model constituted a ply of thickness t. The bottom half is the mirror image of the top section, which represents a second ply. This will be the case for both models, where the composite properties for each configuration and fiber volume ratio will be calculated through equations (7) and (10). The FE analysis will be performed with three $k_f$ combinations for each representative region and under the general assumptions stated beforehand. The moisture load of 1 percent was simulated by calculating the temperature difference ($\Delta T$), given the thermal expansion coefficient and moisture expansion coefficient of each composite section as generated by ICAN. The temperature difference is calculated by the following relation:

$$\Delta T = \frac{\beta_c \Delta M}{\alpha_c} \tag{11}$$

where $\alpha_c$ and $\beta_c$ are the composites's thermal and moisture expansion coefficients, respectively and $\Delta M$ is the change in moisture content which equals 1 percent. The values of $\Delta T$ will vary for each $k_f$ case and they will be used in the FE analysis for the moisture load case. For this study, the selected fiber volume ratios for section 1, region A ($k_{f1}$) will be: 0.50, 0.58, and 0.61. Based on these values of $k_{f1}$, the corresponding $k_{f2}$ values computed from equation (7) are: (a) $k_{f1} = 0.50$ and $k_{f2} = 0.146$, (b) $k_{f1} = 0.58$ and $k_{f2} = 0.17$, (c) $k_{f1} = 0.61$ and $k_{f2} = 0.179$. The values of $k_{f1}$ will correspond

5

to elements with [0/90] composite properties and the $k_{f2}$ values will be assigned to the elements being represented with [+45] and [-45] composite properties. Similarly, the $k_f$ values for elements representing region B are calculated from equation (10). These $k_f$ combinations will be: (a) $k_{f3}$ = 0.35 and $k_{f4}$ = 0, (b) $k_{f3}$ = 0.41 and $k_{f4}$ = 0, (c) $k_{f3}$ = 0.43 and $k_{f4}$ = 0. The three $k_{f1}$ values of 0.50, 0.58, and 0.61 were selected in the range between 0.50 and 0.65. It has been suggested that at these fiber volume ratios the composite's mechanical qualities do not degrade as quickly as with lower fiber contents (ref. 6). This is a significant condition for balanced fabrics subjected to a curing process.

## 4. RESULTS AND DISCUSSION

4.1 Region A: "Cross Over" Region    The application of the pressure and thermal loads affect the through-the-thickness contractions of the woven composite model as follows. The sections of greater epoxy content (section 2) contracted more than the regions of less epoxy content (section 1). This effect is due to the increase in resistance in the thickness direction created by the regions of larger fiber concentration. As the $k_{f1}$ and $k_{f2}$ values were increased from 0.50 and 0.146 to 0.58 and 0.17, there was a reduction in the $\delta$ values from -3.457 to -3.263 mm/m (matrix rich section) and from -0.53 to -0.024 mm/m (fiber rich section). This was expected since the thermal expansion coefficient values are reduced as the fiber content is increased in each section. Even for slight differences in epoxy content such as for $k_{f1}$ = 0.58 and $k_{f2}$ = 0.17 versus $k_{f1}$ = 0.61 and $k_{f2}$ = 0.179, there was a reduction in the normalized displacements from -3.263 to -3.14 mm/m (matrix rich section) and from -0.024 to -0.011 mm/m.

The results obtained from the 1 percent moisture simulation followed a similar pattern. The matrix rich sections of the composite exhibited a greater expansion than the fiber rich sections. The $\delta$ values for the matrix rich sections ($k_{f2}$ = 0.146, 0.17, and 0.179) are equal to 1.324, 1.253 mm/m, and 1.208 mm/m, respectively. The corresponding $\delta$ values for the fiber rich sections ($k_{f1}$ = 0.50, 0.58, and 0.61) are equal to 0.22, 0.026, and 0.017 mm/m, respectively. The restraints placed around the edges of the composite prevented any considerable expansion in the Y direction. Therefore, the contribution of the epoxy matrix towards the through-the-thickness (Z axis direction) expansion was enhanced. The applied restraints were necessary to prevent a nonuniform distribution of the composite under the loads. The $\delta$ values obtained from the curing effects and the hygral load are shown in Table 1 and figures 6(a), 7(a), and 8(a).

The overall effect of the moisture load on the composite surface is to reduce the contractions of the matrix rich sections, created by the applied cure temperature and pressure. The $\delta$ values for the matrix rich sections corresponding to $k_{f2}$ = 0.146, 0.17, and 0.179 are reduced to -2.133, -2.011, and -1.934 mm/m, respectively. The reductions on the fiber rich sections are not significant since the effects of the cure temperature and pressure on these sections are small. These results are shown in figures 6(b), 7(b), and 8(b).

6

## 4.2 Region B: High Matrix Content

The surface contractions developed by the pure matrix sections (section 4) were greater than the ones obtained from the matrix rich sections of region A. The $\delta$ values ranged from -11.315 mm/m for $k_{f3}$ = 0.35 and $k_{f4}$ = 0, up to -11.183 mm/m for $k_{f3}$ = 0.43 and $k_{f4}$ = 0. Since only the fiber volume ratio of section 3 ($k_{f3}$) was increased as $k_{f4}$ remained constant ($k_{f4}$ = 0), the resistance of the fiber rich section to contract or expand will be affected by the pure matrix section. As the pure matrix section contracts (during the cooldown phase of curing), part of the epoxy matrix is displaced into the fiber rich section. This causes the composite section to deform. Similarly, as the pure matrix expands due to the moisture absorption, the epoxy again displaces the neighboring fiber rich composite. As $k_{f3}$ was increased, the contribution from the pure matrix section towards the fiber rich section increased. This is demonstrated from the results obtained for the fiber rich sections ($k_{f3}$ = 0.35, 0.41, and 0.43) under $T_o$ and $P_o$, where the corresponding values are equal to 0.109, 0.139, and 0.144 mm/m. During the 1 percent moisture load, the $\delta$'s obtained from the pure matrix sections are equal to 4.258, 4.195, and 4.173 mm/m. The $\delta$'s corresponding to the fiber rich sections are equal to -0.05, -0.059, and -0.061 mm/m. These results are shown in Table 2 and in figures 9(a), 10(a), and 11(a). This phenomenon did not occurred in region A because there was fiber material present in all of the sections of the model, preventing the epoxy resin from expanding completely. Hence, the effects of the matrix over the total composite was reduced.

The moisture load again reduces the contractions developed by the matrix after the application of the cure temperature and pressure. The normalized displacements for the pure matrix sections corresponding to $k_{f3}$ = 0.35 and $k_{f4}$ = 0, $k_{f3}$ = 0.41 and $k_{f4}$ = 0, $k_{f3}$ = 0.43 and $k_{f4}$ = 0 are: -7.054, -7.017, and -7.006 mm/m, respectively. The corresponding $\delta$'s obtained from the fiber rich sections (section 3) are equal to 0.059, 0.0791, and 0.083 mm/m. These sections were affected by the displaced epoxy of the neighboring matrix sections (section 4), thus the influence of the epoxy upon the fiber rich section was increased as the $k_{f3}$ values were increased from 0.35 up to 0.43. These results are shown in figures 9(b), 10(b), and 11(b).

Based on the results obtained from the FE analysis, the expansion of the epoxy resin was greatly influenced by the cure temperature. From test results on polymeric materials (ref. 7), the glass transition temperature values ($T_g$) ranged from 173 °C (343 °F) up to 211 °C (412 °F). The selected cure temperature of 180 °C (355 °F) falls in that temperature range. This temperature is high enough to initiate the softening of the resin, letting it expand freely and eventually causing the composite to deform. Overall, the dominant factors on the print-through phenomenon of graphite/epoxy woven composites are the resin content and the cure temperature. Since the resin is temperature sensitive to the curing process, the amount of resin in specific sections of the composite can be tailored to reduce the quilting of the surface. Because curing takes place at a specific temperature range, the amount of resin material will be the most significant parameter. This was also the case for the hygral load analysis, in which the resin rich sections were affected more drastically than the fiber rich sections.

7

## 5. PRINT-THROUGH PHENOMENON: PROCEDURE

The procedure used to estimate the print-through of graphite/epoxy woven composites can be summarized as follows:

1. A two-dimensional FE model depicting a cross section of the woven composite system was created. This model represented two different variations corresponding to distinct regions of the plain weave fabric construction. One variation simulated the sections where the fibers cross over one another (region A) while the next variation simulated matrix rich sections of the composite system (region B), (see figures 5(a) and (b)).

2. Given the $k_f$ of a specific section, the fiber volume ratios for each fiber and matrix rich section were calculated through equations (7) and (10).

3. The calculated values of $k_{f2}$ and $k_{f3}$ ($k_{f1}$ is given in this case and $k_{f4} = 0$, matrix only) were substituted into the ICAN code to obtain the corresponding composite material properties for each fiber and matrix rich section. These values were subsequently used to define the material properties in MSC/NASTRAN.

4. The loading and boundary conditions were applied to the FE model as stated in the first three general assumptions, obtaining the top surface normalized displacements ($\delta$). The displacements were normalized with respect to one-half the thickness of the woven composite FE model since there is a contribution from the bottom surface of the model upon the top surface displacements.

5. The percent moisture load effect was simulated by calculating the temperature difference created in each section of the composite model. This value of $\Delta T$ was obtained from equation (11), in which the coefficients of thermal and moisture expansion were computed by ICAN for each $k_f$ case.

## 6. SUMMARY

A computational simulation of surface waviness in graphite/epoxy woven composites due to initial curing and subsequent moisture absorption was presented. The computational simulation reproduced the wrinkles developed on the surface of graphite/epoxy woven composites after a curing process (print-through phenomenon). The simulation was done by creating fiber rich and matrix rich sections in a two-dimensional FE model representing different sections of the woven composite system. These sections were created by assigning the corresponding composite material properties for specific fiber volume ratio combinations. The material properties were generated by the in-house composite mechanics computer code ICAN.

A finite element analysis was performed to obtain the composite's surface normalized displacements based on fiber volume ratios equal to 0.50, 0.58, and 0.61. These $k_f$'s corresponded to the sections of greater fiber concentration in the woven composite (section 1). The $k_f$'s for the adjacent sections (section 2) and for section 3 (fiber rich section of region B) were calculated from the previously given values of $k_{f1}$. The regions of greater epoxy content (sections 2 and 4) contracted/expanded more than the regions of less

8

epoxy content (sections 1 and 3) under the application of thermal, pressure, and hygral loads.  These results demonstrated the strong influence of the epoxy resin on the neighboring sections of the graphite/epoxy woven composite.

# APPENDIX A
## Nomenclature

D        fiber bundle diameter

$k_f$       fiber volume ratio of the composite

l        width of composite section

$l_2$       length of diagonal fiber

M        moisture content

$P_o$       cure pressure

$T_g$       glass transition temperature

$T_o$       cure temperature

t        thickness of composite section (ply thickness)

V        representative volume for each composite section

$V_f$       volume of the fibers in each representative section

$\alpha$       thermal expansion coefficient

$\beta$       moisture expansion coefficient

$\delta$       normalized displacements

## Subscripts

c        composite

f        fiber

o        cure

1,2,3,4   sections 1,2,3,4, respectively

# APPENDIX B

## Constituent Mechanical Properties of AS graphite/EPOXY Matrix Used by ICAN.

| | | | |
|---|---|---|---|
| Number of fibers per end | $N_f$ | 10000 | number |
| Filament equivalent diameter | $d_f$ | $7.62 \times 10^{-3}$ | mm |
| Weight density | $\rho_f$ | 1.74 | $Mg/m^3$ |
| Normal moduli (11) | $E_{f11}$ | 213.74 | GPa |
| Normal moduli (22) | $E_{f22}$ | 13.79 | GPa |
| Poisson's ratio (12) | $\nu_{f12}$ | 0.2 | nondimensional |
| Poisson's ratio (23) | $\nu_{f23}$ | 0.25 | nondimensional |
| Shear moduli (12) | $G_{f12}$ | 13.79 | GPa |
| Shear moduli (23) | $G_{f23}$ | 6.89 | GPa |
| Thermal expansion coef. (11) | $\alpha_{f11}$ | $-9.9 \times 10^{-7}$ | mm/mm K |
| Thermal expansion coef. (22) | $\alpha_{f22}$ | $1.01 \times 10^{05}$ | mm/mm K |
| Heat conductivity (11) | $\kappa_{f11}$ | $1.20 \times 10^4$ | W/m K |
| Heat conductivity (22) | $\kappa_{f22}$ | $1.20 \times 10^3$ | W/m K |
| Heat capacity | $C_f$ | 0.71 | kJ/kg K |
| Fiber tensile strength | $S_{fT}$ | 2757.88 | MPa |
| Fiber compressive strength | $S_{fC}$ | 2757.88 | MPa |

### AS Graphite Fiber Properties

| | | | |
|---|---|---|---|
| Weight density | $\rho_m$ | 1.22 | $Mg/m^3$ |
| Normal modulus | $E_m$ | 3.45 | GPa |
| Poisson's ratio | $\nu_m$ | 0.35 | nondimensional |
| Thermal expansion coef. | $\alpha_m$ | $6.48 \times 10^{-5}$ | mm/mm K |
| Matrix heat conductivity | $\kappa_m$ | 35.27 | W/m K |
| Heat capacity | $C_m$ | 1.05 | kJ/kg K |
| Matrix tensile strength | $S_{mT}$ | 103.42 | MPa |
| Matrix compressive strength | $S_{mC}$ | 172.38 | MPa |
| Matrix shear strength | $S_{mS}$ | 89.63 | MPa |
| Allowable tensile strain | $\epsilon_{mT}$ | $0.20 \times 10^{-2}$ | mm/mm |
| Allowable compr. strain | $\epsilon_{mC}$ | $0.50 \times 10^{-2}$ | mm/mm |
| Allowable shear strain | $\epsilon_{mS}$ | $0.35 \times 10^{-2}$ | mm/mm |
| Allowable torsional strain | $\epsilon_{mTOR}$ | $0.35 \times 10^{-2}$ | mm/mm |
| Void heat conductivity | $k_v$ | 4.67 | W/m K |
| Glass transition temperature | $T_{gdr}$ | 210 | °C |

### Epoxy Matrix Properties

# 7. REFERENCES

1. T.J. Reinhart, et al., Engineered Materials Handbook, Composites, Vol. 1, ASM International, 1987.

2. A.C. Loos, and G.S. Springer, "Curing of Graphite/Epoxy Composites," AFWAL-TR-83-4040, Air Force Wright Aeronautical Laboratories, 1983. (Avail. NTIS, AD-A130071).

3. D.A. Jaworske, Electro-Physics Branch, NASA Lewis Research Center; Private Communication, 1991.

4. H.T. Hahn, and N.J. Pagano, J. Compos. Mater., 9, (1), 91 (1975).

5. P.L.N. Murthy, and C.C. Chamis,"ICAN: Integrated Composite Analyzer," AIAA Paper 84-0974, May 1984.  (Also, NASA TM-83700).

6. P. Paumelle, A. Hassim, and F. Lene, La Recherche Aerospatiale (Engl. Ed.), no. 1, 1 (1990).

7. T.H. Brayden, and C.C. Hays, in Proceedings of the 19th International SAMPE Technical Conference, 598 (1987).

8. S.W. Tsai, Composites Design, Fourth Edition, Think Composites, Dayton, OH, (1988).

9. A.J. Armstrong, et al., J. Mater. Sci., 21, (12) 4289 (1986).

TABLE 1: MAXIMUM AND MINIMUM NORMALIZED DISPLACEMENTS ($\delta$) OF THE
GRAPHITE/EPOXY WOVEN COMPOSITE TOP SURFACE

Region A

| | | $k_{f1} = 0.50$, $k_{f2} = 1.46$ | $k_{f1} = 0.58$, $k_{f2} = 0.17$ | $k_{f1} = 0.61$, $k_{f2} = 0.179$ |
|---|---|---|---|---|
| $\delta_2$, mm/m | Curing effects | -3.457 | -3.263 | -3.140 |
| | 1 percent moisture only | 1.324 | 1.253 | 1.208 |
| $\delta_1$, mm/m | Curing effects | -0.53 | -0.024 | -0.011 |
| | 1 percent moisture only | 0.22 | 0.026 | 0.017 |

NOTE: The subscripts 1 and 2 indicate the section (1 or 2) corresponding to these $\delta$ values.

TABLE 2: MAXIMUM AND MINIMUM NORMALIZED DISPLACEMENTS ($\delta$) OF THE
GRAPHITE/EPOXY WOVEN COMPOSITE TOP SURFACE

Region B

| | | $k_{f3} = 0.35$, $k_{f4} = 0.00$ | $k_{f3} = 0.41$, $k_{f4} = 0.0$ | $k_{f3} = 0.43$, $k_{f4} = 0.00$ |
|---|---|---|---|---|
| $\delta_4$, mm/m | Curing effects | -11.315 | -11.215 | -11.183 |
| | 1 percent moisture only | 4.258 | 4.195 | 4.173 |
| $\delta_3$, mm/m | Curing effects | 0.109 | 0.139 | 0.144 |
| | 1 percent moisture only | -0.050 | -0.059 | -0.061 |

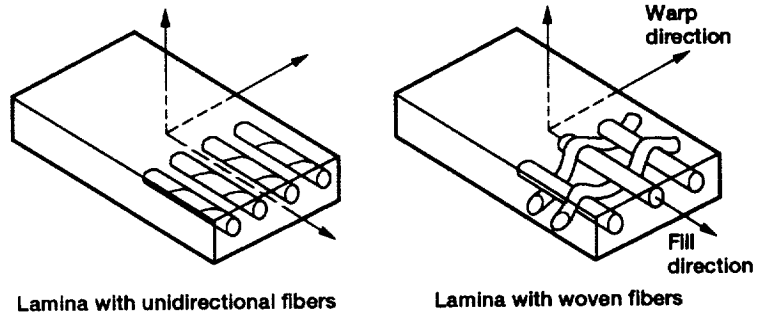NOTE: The subscripts 3 and 4 indicate the section (3 or 4) corresponding to these $\delta$ values.

Lamina with unidirectional fibers          Lamina with woven fibers

Figure 1.—Schematic of lamina with unidirectional fibers versus a lamina with woven fibers.



Note: Delta T = –176 °C

(a) Subjected to a cure pressure of 293.25 kPa and a cure temperature of 180 °C.
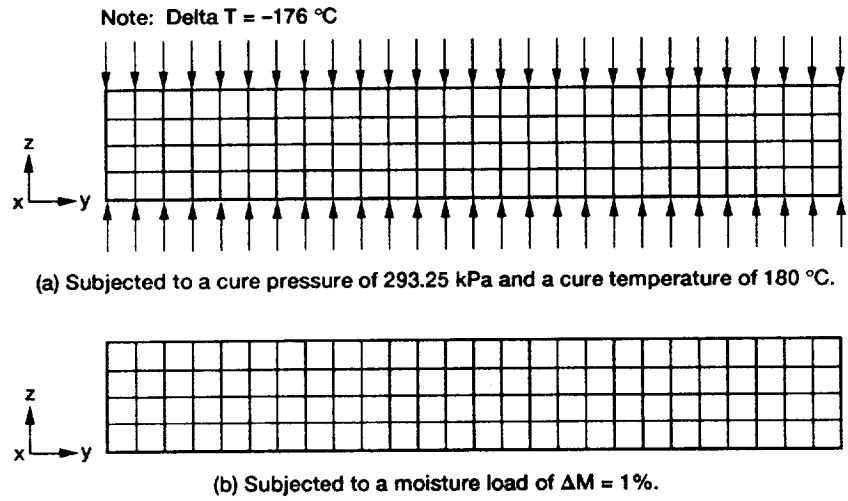
(b) Subjected to a moisture load of $\Delta M$ = 1%.

Figure 2.—Finite element model representing a cross section of the composite model.

14
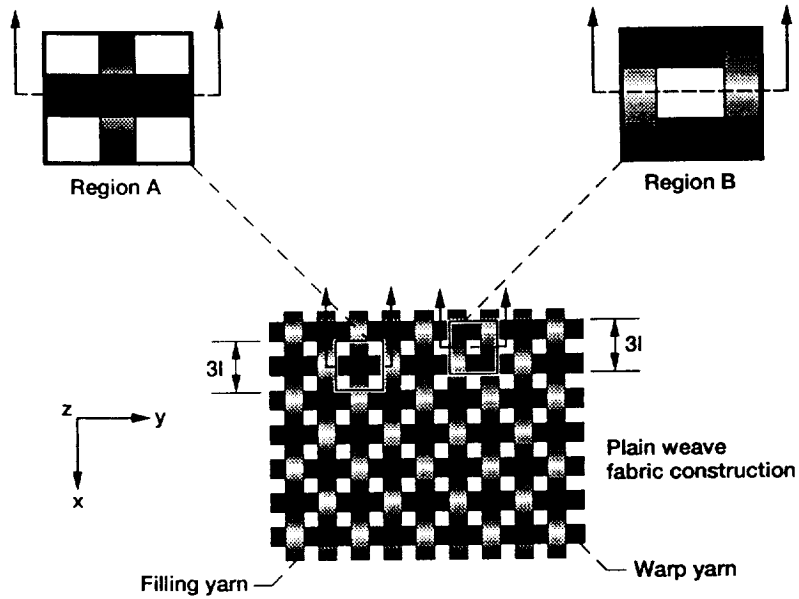
Figure 3.—Schematic of plain weave fabric construction depicting representative regions A and B.
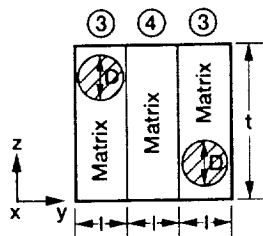
Assumptions:
1. $\gamma = 45°$
2. $l$ = width of each section
3. $t$ = thickness of composite section
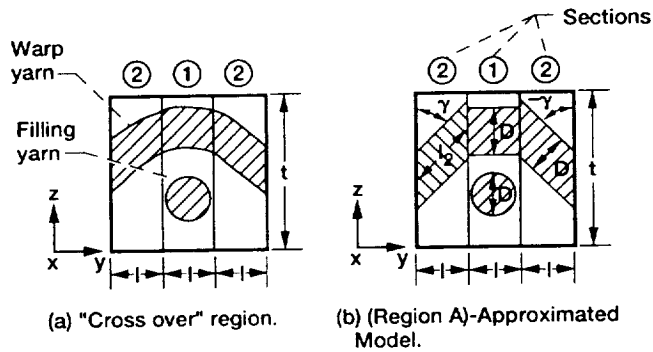


(a) "Cross over" region.

(b) (Region A)-Approximated Model.

(c) (Region B)-High Matrix Content.

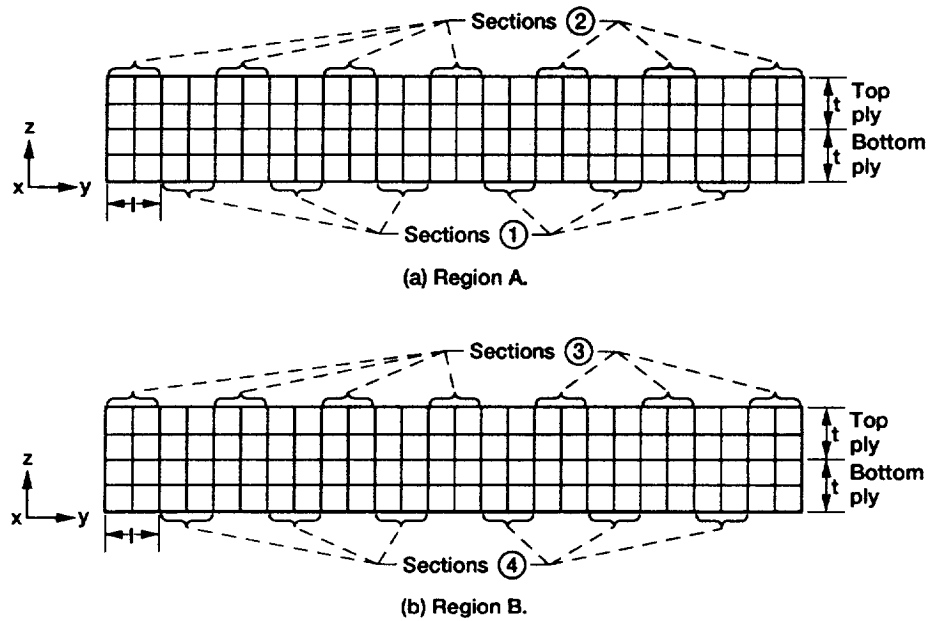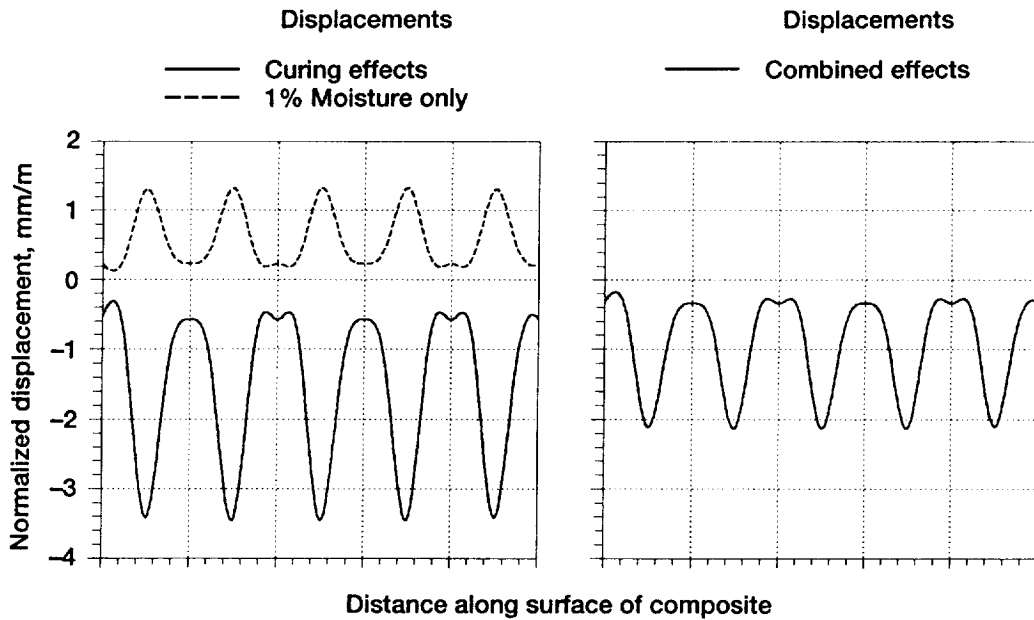Figure 4.—Schematics of woven composite: Region A and region B.

15

(a) Region A.

(b) Region B.

Figure 5.—FE model of alternate cross section.

Surface contractions/expansions after curing and moisture effects on AS/EPOXY woven composites

Displacements

—————— Curing effects
- - - - - 1% Moisture only

Displacements

—————— Combined effects



Distance along surface of composite

(a) $(P_o = 293.25$ kPa, $T_o = 180$ °C) and
$\Delta M = 1\%$.

(b) Combined effects.

Figure 6.—Normalized displacements of top surface for woven composite model, region A-($k_{f1} = 0.50$ and $k_{f2} = 0.146$).

16

Surface contractions/expansions after curing and moisture effects on AS/EPOXY
woven composites

Displacements

——— Curing effects
– – – – 1% Moisture only

Displacements

——— Combined effects

(a) $(P_O = 293.25$ kPa, $T_O = 180$ °C) and
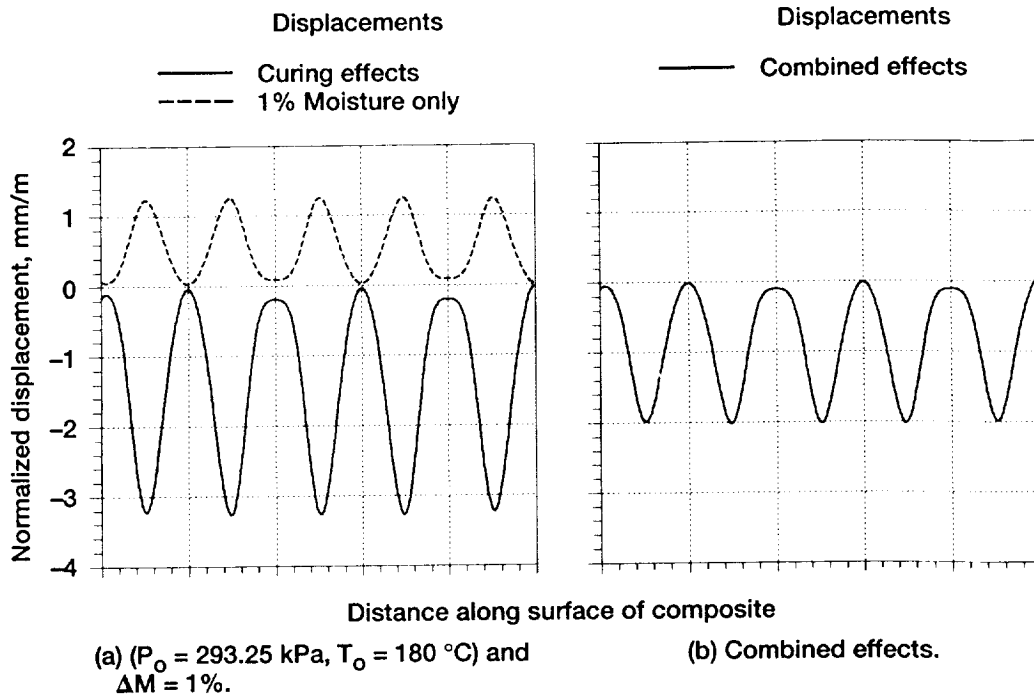$\Delta M = 1\%$.

(b) Combined effects.

Figure 7.—Normalized displacements of top surface for woven composite model, region
A-$(k_{f1} = 0.58$ and $k_{f2} = 0.170)$.

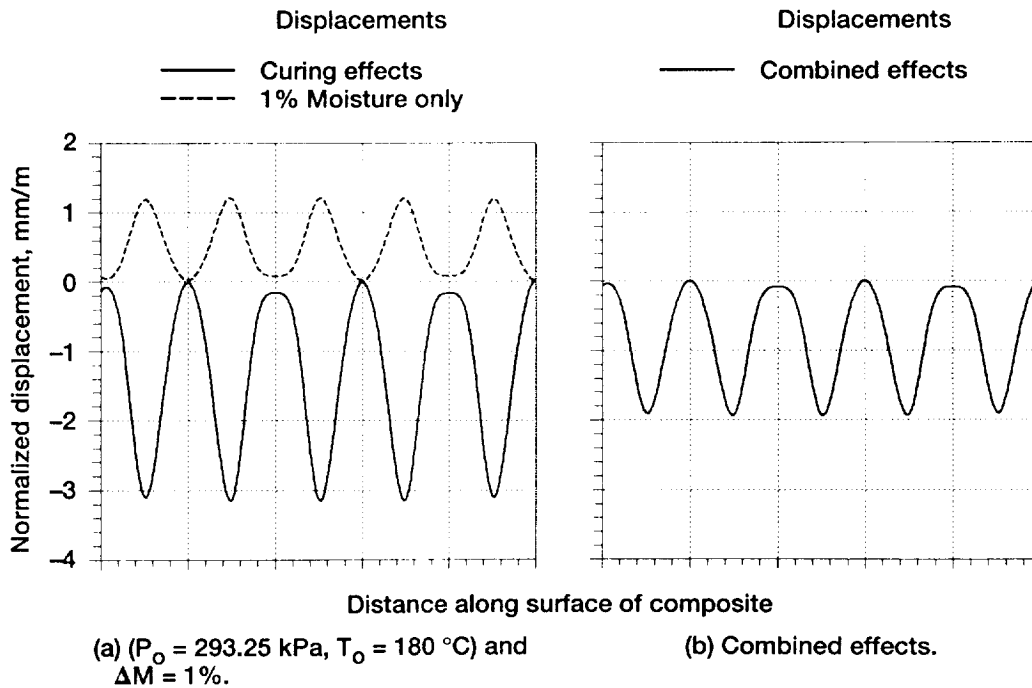Surface contractions/expansions after curing and moisture effects on AS/EPOXY
woven composites

Displacements

——— Curing effects
– – – – 1% Moisture only

Displacements

——— Combined effects

(a) $(P_O = 293.25$ kPa, $T_O = 180$ °C) and
$\Delta M = 1\%$.

(b) Combined effects.

Figure 8.—Normalized displacements of top surface for woven composite model, region
A-$(k_{f1} = 0.61$ and $k_{f2} = 0.179)$.

# REPORT DOCUMENTATION PAGE

Public reporting burden for this collection of information is estimated to average 1 hour per response, including the time for reviewing instructions, searching existing data sources, gathering and maintaining the data needed, and completing and reviewing the collection of information. Send comments regarding this burden estimate or any other aspect of this collection of information, including suggestions for reducing this burden, to Washington Headquarters Services, Directorate for information Operations and Reports, 1215 Jefferson Davis Highway, Suite 1204, Arlington, VA 22202-4302, and to the Office of Management and Budget, Paperwork Reduction Project (0704-0188), Washington, DC 20503.

| 1. AGENCY USE ONLY (Leave blank) | 2. REPORT DATE | 3. REPORT TYPE AND DATES COVERED |
|---|---|---|
| | | Technical Memorandum |

**4. TITLE AND SUBTITLE**

Computational Simulation of Surface Waviness in Graphite/Epoxy Woven Composites Due to Initial Curing

**5. FUNDING NUMBERS**

WU-505-63-5B

**6. AUTHOR(S)**

Jose G. Sanfeliz, Pappu L.N. Murthy, and Christos C. Chamis

**7. PERFORMING ORGANIZATION NAME(S) AND ADDRESS(ES)**

National Aeronautics and Space Administration
Lewis Research Center
Cleveland, Ohio 44135-3191

**8. PERFORMING ORGANIZATION REPORT NUMBER**

E-6666

**9. SPONSORING/MONITORING AGENCY NAMES(S) AND ADDRESS(ES)**

National Aeronautics and Space Administration
Washington, D.C. 20546-0001

**10. SPONSORING/MONITORING AGENCY REPORT NUMBER**

NASA TM-105313

**11. SUPPLEMENTARY NOTES**

Prepared for the 37th International Symposium and Exhibit sponsored by the Society for the Advancement of Material and Process Engineering, Anaheim, California, March 9-12, 1992. Responsible person, Jose G. Sanfeliz, (216) 433-3348.

**12a. DISTRIBUTION/AVAILABILITY STATEMENT**

Unclassified - Unlimited
Subject Category 24

**12b. DISTRIBUTION CODE**

**13. ABSTRACT (Maximum 200 words)**

Several models simulating plain weave, graphite/epoxy woven composites are presented, along with the effects that the simultaneous application of pressure and thermal loads have on their surfaces. The surface effects created by moisture absorption are also examined. The computational simulation consisted of using a two dimensional finite element model for the composite. The properties of the finite element (FE) model are calculated by using the in-house composite mechanics computer code ICAN (Integrated Composite ANalyzer). MSC/NASTRAN is used for the FE analysis which yields the composite's top surface normalized displacements. These results demonstrate the importance of parameters such as the cure temperature ($T_o$) and the resin content in the curing process of polymer-matrix composites. The modification of these parameters will help tailor the composite system to the desired requirements and applications.

**14. SUBJECT TERMS**

Composite materials; Curing; Epoxy resins; Thermal expansion; Moisture

**15. NUMBER OF PAGES**

20

**16. PRICE CODE**

A03

| 17. SECURITY CLASSIFICATION OF REPORT | 18. SECURITY CLASSIFICATION OF THIS PAGE | 19. SECURITY CLASSIFICATION OF ABSTRACT | 20. LIMITATION OF ABSTRACT |
|---|---|---|---|
| Unclassified | Unclassified | Unclassified | |